Three-Dimensional Modeling of Stimulated Brillouin Scattering in Ignition-Scale Experiments

L. Divol, R. L. Berger, N. B. Meezan, D. H. Froula, S. Dixit, L. J. Suter, and S. H. Glenzer

L-399, Lawrence Livermore National Laboratory, University of California, P.O. Box 808, Livermore, California 94551, USA

(Received 16 November 2007; published 24 June 2008)

The first three-dimensional simulations of a high power 0.351 μm laser beam propagating through a high temperature hohlraum plasma are reported. We show that 3D fluid-based modeling of stimulated Brillouin scattering, including linear kinetic corrections, reproduces quantitatively the experimental measurements, provided it is coupled to detailed hydrodynamics simulation and a realistic description of the laser beam from its millimeter-size envelope down to the micron scale speckles. These simulations accurately predict the strong reduction of stimulated Brillouin scattering measured when polarization smoothing is used.

DOI: 10.1103/PhysRevLett.100.255001 PACS numbers: 52.38.Bv, 52.38.Hb, 52.65.Kj

One of the grand challenges of laser-plasma interaction (LPI) studies is to provide guidance for the design of hohlraum targets on the next generation of laser facilities for ignition [1–3]. Modeling LPI processes in real-size experiments has been recognized as a difficult task. One of the main difficulties is the vast parameter space in electron density, temperature, and spatial scales that are typically spanned by an ignition relevant laser-plasma experiment on current laser facilities. This leads to a plethora of (usually coupled) LPI processes such as absorption, refraction, diffraction, filamentation, and parametric backscattering instabilities [4]. Another challenge is the proper description of the spatially smoothed laser beams used on all modern facilities, which exhibit intensity structures from the hundreds of microns down to the micron scale [5].

There are two main numerical modeling approaches for LPI. Particle-in-cell or Focker-Plank type codes solve consistently a set of Maxwell-Vlasov-like equations. While three-dimensional particle-in-cell simulations of diffraction limited short pulse experiments are becoming common tasks due to increasingly powerful computers, long pulse (nanosecond) ignition-scale (cubic millimeter) LPI experiments are still out of reach for such numerical tools. Another approach is to use a fluid-based description of LPI processes [6–9], which has the advantage that both spatial and temporal resolutions are relaxed and no discretization in particle velocity space is required.

In this Letter, we report on the first three-dimensional simulations of a whole laser beam propagating through an ignition-scale experiment, using the fluid paraxial code PF3D. These simulations include models for both stimulated Raman (SRS) and Brillouin (SBS) backscattering. We show that a fluid-based modeling of SBS including linear kinetic correction, coupled to accurate hydrodynamics profiles and a realistic description of the laser intensity pattern generated by various smoothing options, leads to quantitative agreement between the measured and calculated reflectivities over many orders of magnitude and for different smoothing techniques (polarization smoothing and smoothing by spectral dispersion).

We are interested here in validating LPI modeling tools in conditions close to future ignition experiments. In this Letter we model a series of recent experiments [10] performed at the Omega laser facility (LLE, Rochester). An interaction beam propagating along the axis of a hydrocarbon-filled hohlraum heated by up to 17 kJ of heater beam energy interacts with a millimeter-scale underdense ($N_e = 6.5\%$ critical) uniform plasma at electron temperatures T_e around 3 keV. The interaction beam power was varied between 50 and 500 GW, at a wavelength of $\lambda_0 = 0.351$ μm. Using a 150 μm continuous phase plate (CPP), the average intensity on axis was varied between 5×10^{14} W cm^{-2} and 4×10^{15} W cm^{-2}. Absolutely calibrated diagnostics measure the backscattered light. These laser-plasma conditions are close to those encountered in current ignition-hohlraum designs.

First, we need accurate plasma parameters as input for PF3D. Extensive Thomson scattering measurements [11] were successfully compared to HYDRA simulations and show relative insensitivity to the exact heat conduction model employed [12]. We use HYDRA three-dimensional hydrodynamics maps (electron density Ne and temperature T_e, ion temperature T_i, and plasma flow) as initial conditions for PF3D. Figure 1 shows the typical plasma parameters along the hohlraum axis used in the simulation. The transverse variations were also included. We chose to model the experiment at a time when the plasma electron temperature is close to 3 keV and the density profile is relatively uniform.

Second, a realistic description of the laser beam is needed. We use the measured CPP phase mask used on the interaction beam and a model for Omega beam aberrations. Figure 2 shows a 3D rendering of the laser beam propagating through the plasma. The simulation resolves both the envelope of the beam, which is close to a Gaussian with 150 μm FWHM at best focus, and the $f/6.7$ speckles at the micron scale. The typical resolution required by the paraxial approximation used for laser propagation is $dx = dy = 1.3\lambda_0$ and $dz = 4\lambda_0$. The plasma volume modeled encompasses more than 10^9 cells. It is difficult to define an average laser intensity for such a beam, r. As a reference,

the intensity averaged over a 50 μm^3 volume at best focus is 1.15×10^{15} W cm^{-2} for an input power of 100 GW.

Third, the fluid-based code PF3D [9] is used to model the interaction of the laser with the plasma. By coupling a nonlinear hydrodynamics solver with time and/or space enveloped electromagnetic fields it can describe the (nonlinear) evolution of ponderomotive and thermal filamentation, forward Brillouin scattering, and such phenomenon as beam deflection in the presence of transverse flows. These effects can be important in high intensity speckles. In the nonlinear hydrodynamics model [13], the plasma state is completely described by six primitive variables: an ion mass density ρ, the hydrodynamic velocity vector $\mathbf{v}$, and the ion and electron pressures p_i and p_e, respectively. The plasma system consists of five equations expressing mass, momentum, and energy balances coupled to an evolution equation for one of the internal energies:

$$\partial_t \rho + \nabla \cdot (\rho \mathbf{v}) = 0 \qquad \partial_t (\rho \mathbf{v}) + \nabla \cdot (\rho \mathbf{v} \otimes \mathbf{v}) + \nabla p = \mathbf{f}_p$$

$$\partial_t \left(\frac{3}{2} p + \frac{1}{2} \rho |\mathbf{v}|^2 \right) + \nabla \cdot \left[\left(\frac{5}{2} p + \frac{1}{2} \rho |\mathbf{v}|^2 \right) \mathbf{v} \right] = \mathbf{v} \cdot \mathbf{f}_p - \nabla \cdot \mathbf{q} + Q \qquad 3/2[\partial_t p_i + \nabla \cdot (p_i \mathbf{v})] + p_i \nabla \cdot \mathbf{v} = 0,$$

where ρ is the ion mass density, $p = p_e + p_i$ is the total pressure, with $p_e = n_e T_e$ where $n_e = Z\rho/m_i$, Z being the charge state and m_i the ion mass. $\mathbf{f}_p$ is the ponderomotive force of the laser [9], Q represents the laser power absorbed by inverse bremsstrahlung [9], and $\mathbf{q}$ is the electron heat flux [13]. This system is extended to multimaterial plasmas by using tracer variables.

The laser and backscattered light propagation is calculated using the paraxial approximation [9], and the fast plasma response responsible for SBS and SRS is modeled by a linear system of coupled equations for the respective density perturbations. Here we will focus on the details of the current SBS model which was dominant in the experiment. Stimulated Raman backscatter was below measurement threshold for all powers and negligible in simulations too. The electron density perturbation δn associated with the SBS-driven acoustic wave is enveloped in space at $k_a = 2k_0$, but not in time. The resulting differential equation is

$$(\partial_t + u \cdot \nabla + ik_a u_z + \nu_a)^2 \delta n + (\omega_a^2 - 2ik_a c_a^2 \partial_z - c_a^2 \nabla_\perp^2) \delta n = \gamma_a^2 n_e a_0 a_1^* + S, \tag{1}$$

where a_0 (a_1) are the normalized field amplitude of the incoming (backscattered) light ($a \equiv eA/m_e c$). The sound speed is defined as $c_a = \omega_a/k_a$ where ω_a is the acoustic frequency. Numerically, Eq. (1) is solved by factorizing into two coupled first order equations for forward and backward going quantities, with the ponderomotive drive, the volume noise source S, and the transverse diffraction being calculated in split steps. The local acoustic frequency ω_a and Landau damping ν_a are calculated at each position in the plasma by finding the most unstable solution to the Vlasov-Landau kinetic dispersion relation for SBS-driven acoustic waves at $k = k_a$. This is obtained by maximizing $\nu_a^{-1} = \mathrm{Im}(\partial_\omega \epsilon/\epsilon)$, where ϵ is the plasma dielectric function, along the real frequency axis and allows for a correct treatment of multi-ion-species plasma (note that any fluid approximation is bound to fail in hydrocarbon plasmas [14]). At the center of the target, the values are $\omega_a = 13$ ps^{-1} and $\nu_a = 0.15\omega_a$. The coupling coefficient γ_a is obtained by matching the resulting convective amplification to the linear kinetic result. In the fluid limit, $\gamma_a^2 = 4\omega_a^2/[(v_e^2/c^2)(1 + k_a^2 \lambda_{De}^2)]$, but this formula is inaccurate for $k_a \lambda_{De} > 0.5$. This linear kinetic treatment of SBS-

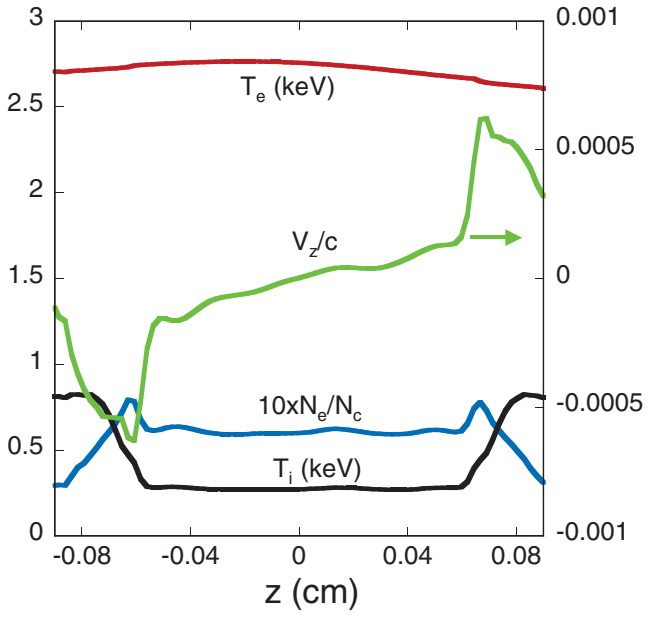

FIG. 1 (color). Plasma parameters at $t = 700$ ps along the hohlraum axis calculated by HYDRA. Electron density, temperature, ion temperature, and flow are used as initial conditions for PF3D simulations.

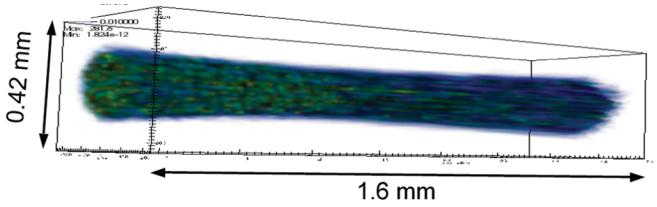

FIG. 2 (color). Three-dimensional rendering of the whole beam as simulated by PF3D.

driven acoustic waves provides a correct description of the time evolution of SBS and recovers the exact steady-state gain exponent, which is necessary for quantitative comparisons with experiments. It is accurate as long as the ion-acoustic wave amplitude is small enough to neglect kinetic and fluid nonlinearities and the electron temperature is high enough to neglect collisional corrections to our kinetic approach (such as nonlocal heat transport). The latter condition is fulfilled in the low density, mid-Z, high temperature experiment (see Fig. 2) described in this Letter, as it is in ignition-hohlraum mid-Z plasmas for all current ignition designs.

Our approach to simulating SBS consists in using 3D hydrodynamics parameters from an integrated HYDRA simulation of the entire hohlraum as initial conditions for PF3D. This is justified by the separation of time scales between the evolution of the gross hydrodynamics simulated by HYDRA (100 ps) and the LPI processes simulated by PF3D (10 ps). The PF3D simulation is then run for a few tens of picoseconds on a plasma volume encompassing the interaction beam, until SBS reaches a statistical steady state. Figure 3 shows that while fast oscillations remains in the reflectivity, a well-defined average emerges after 20 ps for various intensities. We define the PF3D reflectivity as the average between 20 and 50 ps. The fact that we can start the PF3D simulation at 700 ps without prior knowledge of the SBS evolution is justified by an experiment where the interaction beam was delayed by 200 ps and the measured SBS was shown to coincide with the nondelayed measurement [12]: SBS in this hydrocarbon plasma is in the strongly damped regime and reacts almost instantly (over 10 ps) to local laser-plasma conditions. This approach, based on decoupling the large scale hydrodynamic evolution of the target from the LPI physics inside the interaction beam is not always justifiable. In multiple beam experiments, this requires that the LPI physics settles down before significant evolution of the bulk plasma driven by the other beams. While PF3D simulations can be run for hundreds of picoseconds, this limits their usefulness to less than 100 ps runs for our experiment. Also, large reflectivities or strong whole beam self-focusing could modify the large scale hydrodynamic evolution. HYDRA simulations have shown that this is not an issue for this experiment, where the energy of the interaction beam is mostly negligible compared to the 34 heater beams.

Figure 4 shows the measured and simulated SBS reflectivity as function of the interaction beam power. It is worth noting that our modeling does not allow for any free parameter: the laser and plasma parameters used as boundary and initial conditions are given by measurements or integrated simulations validated by measurements, while the SBS model is derived from first-principle linearized equations. The calculated PF3D SBS reflectivities agree quantitatively with measurements over more than 2 orders of magnitude. PF3D predicts correctly the large increase in the SBS threshold when polarization smoothing (PS) is used, as well as the absence of any measurable reduction of

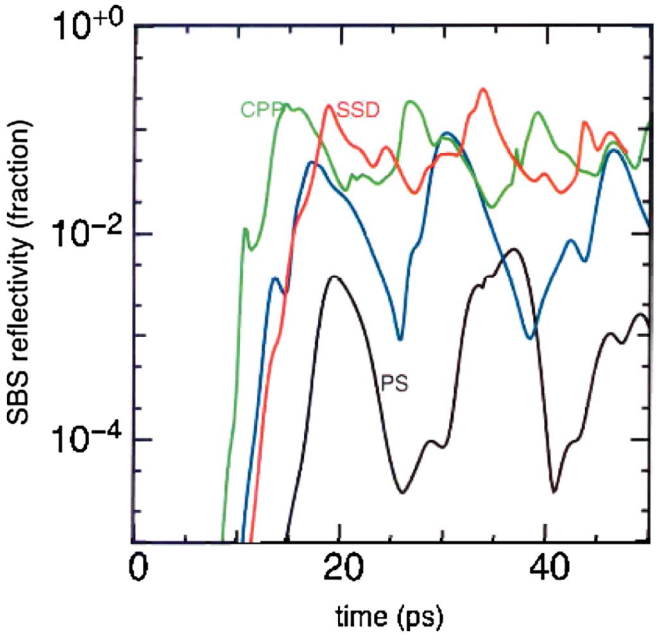

FIG. 3 (color). PF3D calculated SBS reflectivity as function of simulation time for a laser power of 175 GW. Green line is with CPP only, red line is with 3 Å of SSD bandwidth, and black line is with PS. Blue line corresponds to CPP only at 110 GW.

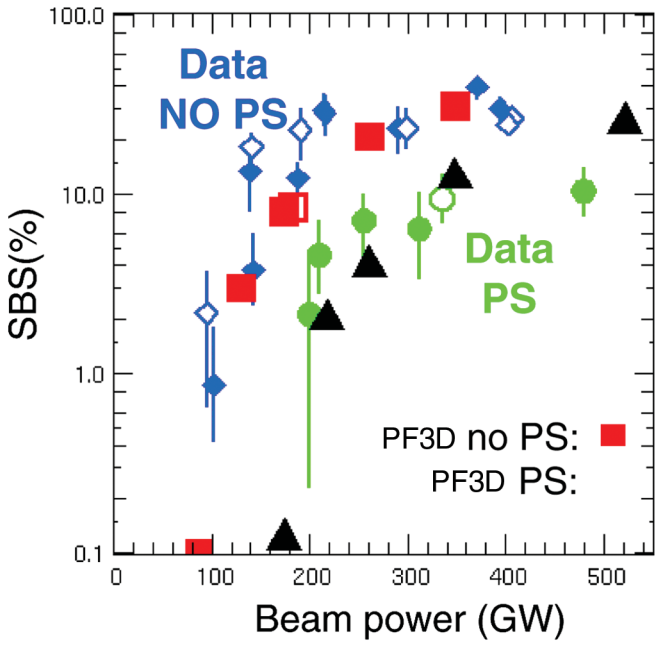

FIG. 4 (color). Measured (blue diamonds and green circles) and calculated (red squares and black triangles) SBS reflectivity as function of laser power at $t = 700$ ps. Both the measurement and simulations show a factor of 2 increase in the SBS threshold when PS is used. Empty symbols correspond to measurements and simulations with 3 Å of SSD added. PF3D results quantitatively match the measured reflectivity for all smoothing techniques employed.

SBS when 3 Å of smoothing by spectral dispersion (SSD) is added. The SBS signal simulated is almost entirely contained in the beam f cone, which is consistent with the experiment. As Fig. 3 shows, the reflectivity oscillates regularly with a period of approximately 12 ps. These oscillations are due to local pump depletion in a few intense speckles in the back of the plasma. The light scattered by these speckles, while representing a modest amount of power, acts as a seed for SBS that is amplified through the plasma. The finite transit time of light through the plasma, coupled to local pump depletion, leads to oscillation in the reflectivity. We turned off the filamentation instability in a few simulations, and while the reflectivity was reduced near threshold, the overall result was very close to Fig. 4.

Thus, the factor of 2 increase in the SBS threshold when PS is used is not due to a control of the filamentation instability [15,16] but to a direct mitigation of the SBS growth. Indeed, the average laser intensity does not exceed the so-called critical intensity for SBS (corresponding to an e-fold amplification over one speckle length) until very large reflectivity is observed. In this regime, the overall reflectivity is determined by amplification over many successive rows of speckles. When PS is used, on average only one or the other polarization is amplified over any speckle, which leads in the limit of small amplification per speckle to a reduction of 2 in the overall gain exponent throughout the whole plasma.

Using 3 Å of SSD bandwidth has no significant effect on SBS, both in the experiment and in simulations. This can be expected in this strongly damped regime where the damping rate ν_a is almost 10 times larger than the inverse correlation time introduced by the laser bandwidth. The situation could be quite different in a weakly damped regime, such as in the gold plasma close to the hohlraum wall [17]. Previous observations of SBS reduction through control of filamentation by SSD does not apply to this high-T_e, moderate intensity experiment, as noted before.

The validity of our description of SBS-driven ion-acoustic waves relies on their amplitude remaining small. To quantify this, we have computed the distribution of the wave amplitude $\delta n/n_e$ for a laser power of 150 GW (CPP only) when a reflectivity of about 8% was calculated. We find that less than 1% of the simulation volume is occupied by waves with amplitudes above 0.3%. The maximum amplitude observed is 3%. Fluid nonlinearities scale usually with $(\delta n/n_e)^2$ and are thus negligible [18]. These amplitudes are also well below the two-ion decay instability threshold [19] and the wave-breaking limit. Trapping of electron (or H ions) could lead to a frequency shift [20] (a 1% effect for $\delta n/n_e = 0.3\%$, thus negligible) and a reduction of Landau damping in intense speckles for $\delta n/n_e$ as low as 0.3% with the parameters of Fig. 1. This last effect could limit the validity of our SBS model above 150 GW for CPP only (and above 300 GW for CPP + PS), but as reflectivities are already large and the physics is dominated by whole-beam pump depletion, the experimental measurement is not discriminative.

While developing a general predictive modeling capability for LPI remains a challenge, we have made a significant step towards that goal by using a detailed description of the plasma conditions and the laser beam intensity pattern as input to full 3D fluid-based LPI simulations. This approach relies on the separation of scale (time, space, and energy) between the LPI processes taking place inside the interaction beam and the overall hydrodynamics evolution of the surrounding plasma. This numerical modeling approach is scalable to National Ignition Facility (NIF) size plasmas with current supercomputers (i.e., the simulation volume would increase from 0.5 to 10 mm^3 and the number of computing units from 512 to 10 000). A needed improvement for NIF ignition-hohlraum simulations would be a feedback mechanism to couple these different scales. This experimental validation is for now limited to stimulated Brillouin backscatter in a regime where kinetic and fluid nonlinearities are not expected to play a significant role (long hot plasma at moderate density and laser intensity). This is a regime of interest for forthcoming attempts at ignition on NIF and Laser MegaJoule (LMJ).

This work was performed under the auspices of the U.S. Department of Energy by Lawrence Livermore National Laboratory in part under Contract No. DE-AC52-07NA27344.

[1] E. I. Moses and C. R. Wuest, Fusion Sci. Technol. **47**, 314 (2005).
[2] C. Cavailler, Fusion **47**, B389 (2005).
[3] J. D. Lindl *et al.*, Phys. Plasmas **11**, 339 (2004).
[4] W. L. Kruer, *The Physics of Laser Plasma Interaction* (Addison-Wesley, New York, 1988).
[5] C. H. Still *et al.*, Phys. Plasmas **7**, 2023 (2000).
[6] S. Huller, Ph. Mounaix, and D. Pesme, Phys. Scr. **T63**, 151 (1996).
[7] A. J. Schmitt and B. B. Afeyan, Phys. Plasmas **5**, 503 (1998).
[8] J. Myatt *et al.*, Phys. Plasmas **11**, 3394 (2004).
[9] R. L. Berger *et al.*, Phys. Plasmas **5**, 4337 (1998).
[10] D. H. Froula *et al.*, Phys. Rev. Lett. **98**, 085001 (2007).
[11] D. H. Froula *et al.*, Phys. Plasmas **14**, 055705 (2007).
[12] N. B. Meezan *et al.*, Phys. Plasmas **14**, 056304 (2007).
[13] J. A. F. Hittinger and M. R. Dorr, J. Phys.: Conf. Ser. **46**, 422 (2006).
[14] E. A. Williams *et al.*, Phys. Plasmas **2**, 129 (1995).
[15] E. Lefebvre *et al.*, Phys. Plasmas **5**, 2701 (1998).
[16] S. H. Glenzer *et al.*, Nature Phys. **3**, 716 (2007).
[17] L. Divol, Phys. Rev. Lett. **99**, 155003 (2007).
[18] W. Rozmus *et al.*, Phys. Fluids B **4**, 576 (1992).
[19] C. Niemann *et al.*, Phys. Rev. Lett. **93**, 045004 (2004).
[20] C. Riconda *et al.*, Phys. Rev. Lett. **94**, 055003 (2005).